Journal of Electrochemical Science and Technology
Vol. 2, No. 4, 2011, 187-192
http://dx.doi.org/10.5229/JECST.2011.2.4.187

Journal of Electrochemical Science and Technology

Photoelectrochemical Water Oxidation Using ZnO Nanorods Coupled with Cobalt-Based Catalysts

Tae Hwa Jeon[a], Sung Kyu Choi[b], Hye Won Jeong[c], Seungdo Kim[d], and Hyunwoong Park[c,†]
[a]*Department of Energy Science*
[b]*Department of Physics*
[c]*School of Energy Engineering, Kyungpook National University, Daegu 702-701, Korea*
[d]*Deptartment of Environmental Science and Biotechnology, Hallym University, Chuncheon 200-702, Korea*

ABSTRACT

Photoelectrochemical performances of ZnO electrodes are enhanced by coupling with cobalt-based catalyst (CoPi) in phosphate electrolyte (pH 7). For this study, hexagonal pillar-shaped ZnO nanorods are grown on ZnO electrodes through a chemical bath deposition, onto which CoPi is deposited with different photodeposition times (10-30 min). A scanning electron microscopic study indicates that CoPi deposition does not induce any change of ZnO morphology and an energy-dispersive X-ray spectroscopic analysis shows that inorganic phosphate ions (Pi) exist on ZnO surface. Bare ZnO electrodes generate the current of ca. 0.36 mA/cm^2 at a bias potential of 0.5 V vs. SCE, whereas ZnO/CoPi (deposited for 10 min) has ca. 50%-enhanced current (0.54 mW/cm^2) under irradiation of AM 1.5G-light (400 mW/cm^2). The excess loading of CoPi on ZnO results in decrease of photocurrents as compared to bare ZnO likely due to limited electrolyte access to ZnO and/or CoPi-mediated recombination of photogenerated charge carriers. The primary role of CoPi is speculated to trap the photogenerated holes and thereby oxidize water into molecular oxygen via an intervalency cycle among Co(II), Co(III), and Co(IV).

Key words: Artificial photosynthesis, Solar hydrogen, Electrocatalyst, Water splitting, Semiconductors

Received November 29, 2011 : Accepted December 13, 2011

1. Introduction

As demand for carbon-neutral fuels continually increases, the photoelectrochemical (PEC) production of chemical fuels has received much attention.[1-3] The PEC water oxidation is a valuable reaction for producing solar fuels such as molecular hydrogen and methanol from proton and carbon dioxide, respectively (reactions 1-3).

$$2H_2O \rightarrow O_2 + 4H^+ + 4e^- \quad (1)$$

$$2H^+ + 2e^- \rightarrow H_2 \quad (2)$$

$$CO_2 + 6H^+ + 6e^- \rightarrow CH_3OH + H_2O \quad (3)$$

Various semiconductor electrodes have been demonstrated to intrinsically induce the PEC water oxidation,[4-9] yet most of them still suffer from low photoconversion efficiencies primarily due to rapid charge recombination and poor catalytic effect for driving multi-electron transfers at interface.[10] Several noble metal-based catalysts (e.g., Pt, RuO_2) have been coupled to semiconductors to hurdle such the kinetically hindered water oxidation and simultaneous evolution of molecular oxygen.[11] However, their high costs limit the widespread application. Very recently, cobalt(II)-photosphate complexes (CoPi) have been reported to successfully catalyze the oxidation of water into molecular oxygen with high efficiency

†Corresponding author. Tel.: +82-53-950-7371
E-mail address: hwp@knu.ac.kr

relatively at low overpotentials in phosphate-buffered water of circum-neutral pH.[12] The molecular structure, catalytic mechanism, and stability of the CoPi have been studied in detail.[12-14] Although not fully disclosed, the structure of CoPi is speculated to likely be of molecular dimension with composition of edge-sharing CoO_6 octahedara and a Co : P of 2 : 1 or 3 : 1. When catalyzing water oxidation, CoPi undergoes proton-coupled electron transfers along with cyclic valency changes between Co(II/III) and Co(III/IV).

It has been demonstrated that the PEC water oxidation performances of semiconductor electrodes are significantly enhanced by a factor of over two when CoPi was electrodeposited onto semiconductor electrodes.[15-21] In this reaction, the primary role of CoPi is to facilitate the photogenerated hole transfers via an intervalency cycle of Co(II), Co(III), and Co(IV). However, the electrodeposition grows the CoPi very rapidly, forming a thick layer that fully covers the underlying semiconductor particles. Under this condition, the access of electrolytes to the semiconductor surface is highly limited.[8] Instead of electrodeposition, therefore, photo-assisted deposition (photodeposition) was employed to couple between semiconductor and CoPi.[8,16,17]

The purpose of this study is to examine that CoPi can be photodeposited on ZnO electrode and if so, how much the PEC performance of ZnO electrode can be enhanced by deposited CoPi. ZnO has diverse advantages such as high chemical stability[22] and relatively easy synthesis of one-dimensional nanoarchitectures (e.g., nanowire, nanobowls, and nanorods).[2-5] In this study, ZnO nanorods were fabricated on conducing glass electrodes by a chemical bath deposition, over which CoPi was photodeposited.

2. Experimental

2.1. Preparation of ZnO/CoPi Electrodes

ZnO electrodes were prepared by following a chemical bath deposition process reported elsewhere.[23] In detail, fluorine-doped SnO_2 (FTO) glass (F:SnO_2, Pilkington Co., TEC7) was cleansed with ethanol for 10 minutes in an ultrasound bath, rinsed with distilled water, and dried at room temperature. Zinc acetate ($Zn(O_2CCH_3)_2$, Aldrich) was dissolved in ethanol (99.0%, Aldrich) at 5 mM, 0.2 mL of which was dropped on FTO glass and spin-spread at 1000 rpm for 6 seconds (repeated over three times). After dried at room temperature, the electrodes were annealed at 250°C for 30 minutes. This casting-drying-annealing process was cycled twice to obtain robust films. Then, as-obtained ZnO electrodes were immersed for 3 hours in a mixed solution of zinc nitrate ($Zn(NO_3)_2$) (0.1 M) and hexamethylenetetramine ($(CH_2)_8N_4$). During the immersion process, the solution temperature was maintained at 93°C. Finally, ZnO electrode was rinsed with distilled water and dried. Cobalt phosphate complexes (CoPi) were loaded on ZnO electrodes by a photodeposition process. As-prepared ZnO electrodes were immersed in 0.1 M potassium phosphate buffer solution with 0.5 mM $CoCl_2$. A simulated solar light (AM 1.5, 4 Sun) was irradiated to ZnO electrodes through the solution using a 150-W Xenon arc lamp (Ushio 150-MO) for different times. After being washed with distilled water and dried under air, the electrodes were kept in the dark.

2.2. Surface Characterization and Photoelectrochemical Tests

The surfaces of ZnO and ZnO/CoPi electrodes were analyzed by a field emission scanning electron microscope (FE-SEM, Hitachi S-4800) equipped with energy-dispersive X-ray spectroscopy (EDX). Photoelectrochemical study of ZnO/CoPi electrodes were performed in a three-electrode system in 0.1 M potassium phosphate buffer with a graphite rod and a saturated calomel electrode (SCE) as a counter and a reference electrode, respectively. For linear sweep voltammograms, potentials were applied from –0.5 V to +1.5 V vs. SCE with a scan rate of 0.1 V/s using a potentiostat (Versastat 3-400). Time-profiled photocurrents were obtained at various constant potentials (0.2, 0.5, and 1.0 V vs. SCE). A 150-W Xenon arc lamp (Ushio 150-MO) equipped with an AM 1.5G filter (400 mW/cm^2) was used as light source.

3. Results and Discussion

3.1. Surface Analysis and Photoelectrochemical Behaviors

Fig. 1 shows the SEM images of bare ZnO (a, b) electrodes and ZnO/CoPi electrodes (c, d). ZnO has flower-like images that are composed of many nanorods (hexagonal pillars) of ca. 300 nm in diameter and a few micron-meters in size. It is apparent that each nanorod grows from ZnO film indicating the underlying ZnO acts as a seed for the nanorods. The SEM images of ZnO/CoPi (deposited for 10 min) were also taken, yet the overall images seemed to be very similar to those of bare ZnO (Fig. 1(c), (d)). However, a detailed comparison between the two nanorods (Fig. 1(d) inset for ZnO vs.

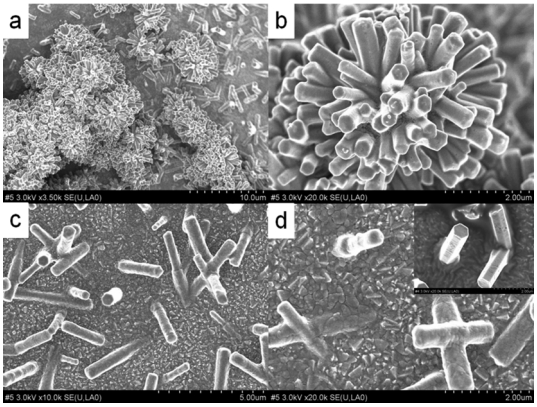

Fig. 1. SEM images of (a, b) bare ZnO electrodes and (c, d) ZnO/CoPi (deposited for 10 min) electrodes. Fig. 1(d) inset shows the bare ZnO nanorods for comparison with ZnO/CoPi.

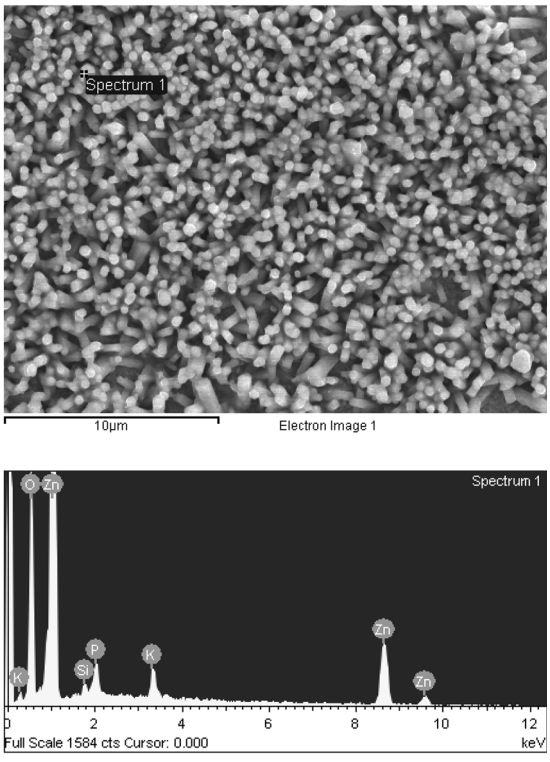

Fig. 2. EDX analysis of ZnO/CoPi electrode. CoPi was photodeposited for 10 min.

Fig. 1(d) for ZnO/CoPi) indicates that ZnO nanorods have a clean and flat surface whereas the surface of CoPi-deposited nanorods is bumpy and rather rough. According to previous reports,[8,16,18] electrodeposited CoPi exhibited a very thick film or overlayer on semiconductor electrodes, whereas photodeposited CoPi formed a very thin layer being difficult to identify the deposited CoPi.[8] In order to find evidence for CoPi, ZnO/CoPi electrode was analyzed with EDX. As shown in Fig. 2, the EDX results indicate that zinc and oxygen are the main constituents. Cobalt was not detected likely due to minor content whereas potassium was observed at 2.27 % (Table 1), indicative of CoPi.

Fig. 3(a) shows linear sweep voltammograms of bare ZnO and ZnO/CoPi electrodes as a function of photodeposition time for CoPi in the absence (a-d) and presence (a'-d') of light. Bare ZnO electrode showed virtually no electrocatalytic activity in the absence of light (a) and generated current at around ca. –0.1 V vs. SCE upon irradiation (a'). The valence band level of ZnO (2.952 V vs. SCE) is highly positive of water oxidation potential (0.99 V vs. SCE) and the photogenerated holes of ZnO could intrinsically oxidize water into molecular oxygen (Scheme 1). When CoPi was photodeposited for 10 min, ZnO/CoPi electrode exhibited much enhanced photocurrent generation despite similar onset potential with around –0.15 V (b'). Other ZnO/CoPi electrodes with longer photodeposition times (20 and 30 min) also showed similar photoelectrochemical responses (c' and d'). It should be pointed that ZnO/CoPi electrodes have high electrocatalytic activities even in the dark, which increased with increasing the photodeposition time (b-d). Upon deposition, the valency of cobalt was reported to be mixed with +2 and +3, and the potential for $Co^{3+/2+}$ is around 1.58 V vs. SCE, much positive of the water oxidation potential (Scheme 1). To avoid the effect of underlying ZnO, therefore, CoPi was electrodeposited on bare FTO glass electrodes and their electrochemical behaviors were examined in the absence and presence of light (Fig. 3(b)). FTO/CoPi generated a significantly large amount of current from at around 1.23 V vs. SCE, indicating that CoPi itself is a highly active water oxidation electrocatalyst. It was found that CoPi has no effect of irradiation and thus all the enhanced photocurrents of ZnO/CoPi should

Table 1. EDX analysis of ZnO/CoPi (deposited for 10 min) electrode

Element	O	Si	P	K	Zn
Atomic %	55.93 ± 0.99	0.92 ± 0.17	2.27 ± 0.18	2.15 ± 0.17	38.73 ± 1.17

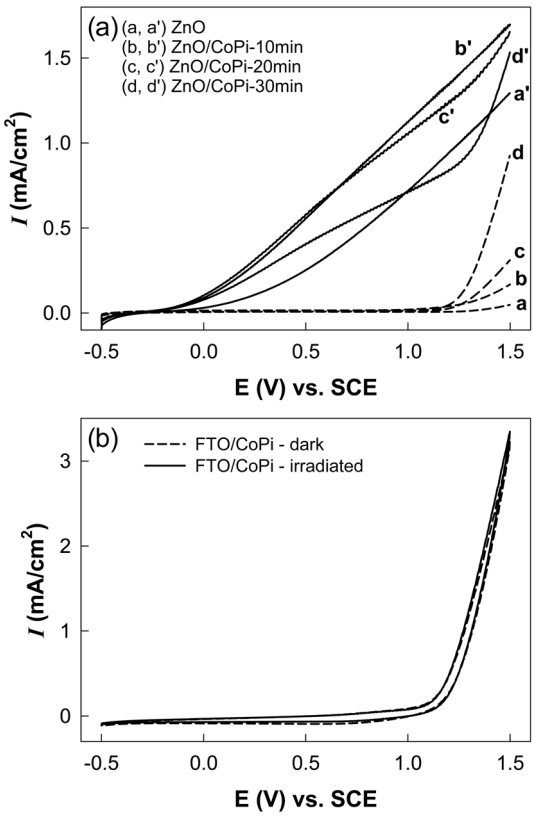

Fig. 3. (a) Linear sweep voltammograms of bare ZnO electrodes (a, a') and ZnO/CoPi electrodes (b-d & b'-d') as a function of photodeposition time in the dark (a-d) and under irradiation (a'-d'). (b) Cyclic voltammograms of bare CoPi electrodes (deposited on FTO) in the dark and under irradiation. Electrolytes: 0.1 M potassium phosphate buffer (pH 7). Scan rate: 0.1 V/s.

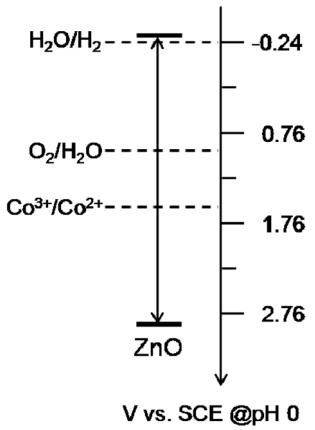

Scheme 1. Energy levels for key components in ZnO/CoPi system.

come from photoelectrochemical reaction of ZnO.

We have also examined the photocurrent generation at E = 0.2 V vs. SCE upon light on and off (Fig. 4(a)). Upon irradiation, bare ZnO electrode generated the current of ca. 0.13 mA/cm^2 and ZnO/CoPi (deposited for 10 min) had around 1.5-fold enhanced current. The positive effect of CoPi was observed even at higher potentials of 0.5 and 1.0 V. It is interesting that the photoelectrochemical performance of ZnO/CoPi is reduced and even lower than bare ZnO when the photodeposition time increases up to 30 min. This indicates that the excess amount of CoPi induces the negative effect likely due to CoPi-mediated recombination (see below). Alternatively, the excess amount of CoPi can block the facile access of electrolyte into the underlying ZnO, inhibiting the electric communication between the ZnO and the electrolyte.

3.2. Reaction Mechanism of ZnO/CoPi Electrodes

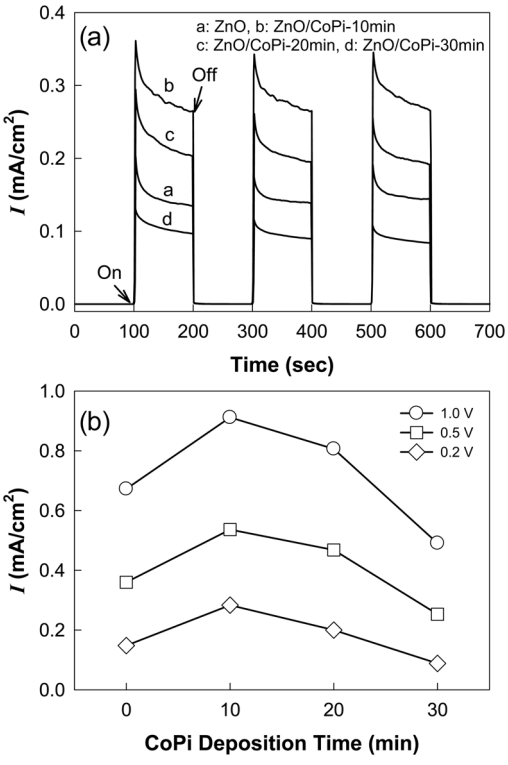

Fig. 4. (a) Time-profiled current generation of ZnO/CoPi electrodes with different photodeposition times upon light on and off. E = 0.2 V vs. SCE. (b) Effect of CoPi photodeposition times on the photocurrent generations at E = 0.2, 0.5, and 1.0 V vs. SCE. Electrolyte: 0.1 M potassium phosphate buffer (pH 7).

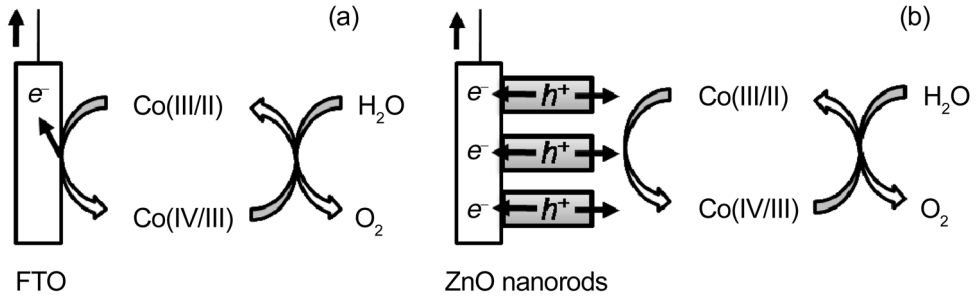

Scheme 2. Schematic illustration for charge transfer mechanism of (a) FTO/CoPi and (b) ZnO/CoPi electrodes.

Scheme 2 shows the overall water oxidation mechanism of CoPi electrode (a: coated on FTO) and ZnO/CoPi electrode (b). During the deposition process on substrates via electrodeposition or photodeposition, the valence state of cobalt ion (Co(II)) becomes partially oxidized into the mixed state of Co(II) and Co(III). When anodic bias potentials are applied to FTO/CoPi, cobalt ions are oxidized into the mixed state of Co(IV/III) (Scheme 2(a)). Due to high reduction potential, Co(IV/III) is rapidly reduced back to the original state accompanying the simultaneous oxidation of water into molecular oxygen. In this regard, CoPi acts as the water oxidation electrocatalyst. In the case of ZnO/CoPi, irradiation creates electron-hole pairs at ZnO; electrons are transported away from ZnO electrode due to applied potential while holes oxidize Co(III/II) into Co(IV/III) (Scheme 2b). The valence band hole of ZnO can directly oxidize water yet the ZnO surface seems to have lower catalytic effect (or sites) for direct water oxidation. On the other hand, Co(III/II) can rapidly trap the holes, enhancing the charge separation and resultantly increasing the photocurrent. However, if there is the excess amount of CoPi, the Co(IV/III) traps the photogenerated electrons. In this case, CoPi acts as a recombination site reducing the overall photoelectrochemical performance.

Thermodynamically, the oxidation power of Co(IV/III) is very strong enough to oxidize water (Scheme 1). However, the charge transfer kinetics may be a different issue. Unfortunately, no kinetic study on the charge transfers at ZnO/CoPi has been performed. Instead, we can infer the effect of CoPi on the charge transfers (i.e., hole transfer) from other semiconductor electrodes coupled with CoPi. For example, CoPi increased the lifetime of photogenerated holes in α-Fe_2O_3 electrode by more than three orders of magnitude without any potential bias.[24] Taking into account that the lifetime of photogenerated holes at α-Fe_2O_3 is around 3 seconds at a positive bias potential,[25] a similar or longer lifetime of the holes can be expected with CoPi deposit. In ZnO/CoPi system, the enhanced photocurrents, therefore, may result not only from the high oxidation power of CoPi but also from the kinetically long-lived holes (or electrons).

4. Conclusion

This study demonstrated that the photoelectrochemical performance of ZnO electrodes could be enhanced significantly simply by coupling with CoPi electrocatalyst. It was found that the current generation was increased by CoPi deposit by a factor of around 1.5. Despite difficulty in providing the direct evidence for existence of cobalt ion on ZnO surface, EDX analysis for phosphate and electrocatalytic performance of ZnO/CoPi in the dark should support the existence of CoPi deposit. In the role of CoPi, the intervalency cycle of Co(IV/III/II) was presumed as a primary mechanism for enhancing the photoelectrochemical performance of ZnO electrode.

Acknowledgements

This research was supported by the Basic Science Research Programs (No. 2010-0002674 and 2011-0021148) through the National Research Foundation of Korea (NRF) funded by the Ministry of Education, Science and Technology.

References

1. A.J. Bard and M.A. Fox, *Acc. Chem. Res.*, **28**, 141 (1995).
2. T.R. Cook, D.K. Dogutan and S.Y. Reece, Y. Surendranath, T.S. Teets and D.G. Nocera, *Chem. Rev.*, **110**, 6474 (2010).
3. M.G. Walter, E.L. Warren, J.R. Mckone, S.W. Boettcher, Q. Mi, E.A. Santori and N.S. Lewis, *Chem. Rev.*, **110**,

6446 (2010).
4. P.H. Borse, H. Jun, S.H. Choi, S.J. Hong and J.S. Lee, *Appl. Phys. Lett.*, **93**, 173103 (2008).
5. F.L. Souza, K.P. Lopes, E. Longo and E.R. Leite, *Phys. Chem. Chem. Phys.*, **11**, 1215 (2009).
6. H. Wang, T. Lindgren, J. He, A. Hagfeldt and S.E. Lindquist, *J. Phys. Chem. B*, **104**, 5486 (2000).
7. W.J. Youngblood, S.H.A. Lee, Y. Kobayashi, E.A. Hernandez-Pagan, P.G. Hoertz, T.A. Moore, A.L. Moore, D. Gust and T.E. Mallouk, *J. Am. Chem. Soc.*, **131**, 926 (2009).
8. T.H. Jeon, W. Choi and H. Park, *Phys. Chem. Chem. Phys.*, DOI: 10.1039/c1031cp23135a (2011).
9. A. Bak, W. Choi and H. Park, *Appl. Catal. B*, **110**, 207 (2011).
10. K. Sivula, F.L. Formal and M. Graetzel, *ChemSusChem*, **4**, 432 (2011).
11. S. Trasatti (1980) *Electrodes of conductive metal oxides*, Elsevier, New York.
12. M.W. Kanan and D.G. Nocera, *Science*, **321**, 1072 (2008).
13. M.W. Kanan, Y. Surendranath and D.G. Nocera, *Chem. Soc. Rev.*, **38**, 109 (2009).
14. J.G. McAlpin, Y. Surendranath, M. Dinca, T.A. Stich, S.A. Stoian, W.H. Casey, D.G. Nocera and R.D. Britt, *J. Am. Chem. Soc.*, **132**, 6882 (2010).
15. E.M.P. Steinmiller and K.S. Choi, *Proc. Natl. Acad.*, **106**, 20633 (2009).
16. K.J. McDonald and K.S. Choi, *Chem. Mat.*, **23**, 1686 (2011).
17. D.K. Zhong, M. Cornuz, K. Sivula, M. Graetzel and D.R. Gamelin, *Energy Environ. Sci.*, **4**, 1759 (2011).
18. D.K. Zhong and D.R. Gamelin, *J. Am. Chem. Soc.*, **132**, 4202 (2010).
19. J.J.H. Pijpers, M.T. Winkler, Y. Surendranath, T. Buonassisi and D.G. Nocera, *Proc. Nat. Acad. Sci.*, **108**, 10056 (2011).
20. J.A. Seabold and K.S. Choi, *Chem. Mater.*, **23**, 1105 (2011).
21. E.R. Young, R. Costi, S. Paydavosi, D.G. Nocera and V. Bulovic, *Energy Environ. Sci.*, 2058 (2011).
22. J.C. Johnson, K.P. Knutsen, H.Q. Yan, M. Law, Y.F. Zhang, P.D. Yang and R.J. Saykally, *Nano Lett.*, **4**, 197 (2004).
23. L.L. Yang, Q.X. Zhao and M. Willander, *J. Alloy. Compd.*, **469**, 623 (2009).
24. M. Barroso, A.J. Cowan, S.R. Pendlebury, M. Gratzel, D.R. Klug and J.R. Durrant, *J. Am. Chem. Soc.*, **133**, 14868 (2011).
25. S.R. Pendlebury, M. Barroso, A.J. Cowan, K. Sivula, J. Tang, M. Gratzel, D.R. Klug and J.R. Durrant, *Chem. Commun.*, **47**, 716 (2011).